

Journal of Mechanics of Materials and Structures

**A NOTE ON WEAR OF ELASTIC SLIDING PARTS
WITH VARYING CONTACT AREA**

Michele Ciavarella and Nicola Menga

Volume 10, No. 3

May 2015



A NOTE ON WEAR OF ELASTIC SLIDING PARTS WITH VARYING CONTACT AREA

MICHELE CIAVARELLA AND NICOLA MENGA

Wear of sliding parts in the transient regime depends on elastic behavior of the bulk of the materials, and in general the contact area cannot be assumed to be constant, so that the problem is nonlinear. Here we look at the simple example of the classical Hertzian geometry, obtaining a simple solution for transient to uniform pressure (which is also the “rigid” limit solution) assuming out-of-plane sliding, and the approximation of the “Winkler foundation” in plane strain. Wear is assumed to vary according to the Reye–Archard law, which applies locally and only to the wearing indenter. As a further improvement, we give a more refined solution using a Winkler constant which adapts to the changing size of the contact.

1. Introduction

Wear, together with fatigue, is one of the major causes of malfunctioning and disservice of engineering components. As such, the literature on wear is huge, particularly on the experimental side. Well known are Ashby’s wear maps [Lim and Ashby 1987], which fit a large number of experiments and permit estimation of different regimes of wear, which depend on temperature at the interface and in the bulk, and, correspondingly, the orders of magnitude of variation in the wear coefficient, mainly dependent on pressure and relative speed.

Even for a constant speed, we generally distinguish two different phases: “running-in”, in which transient processes occur, and “steady state”. It should be remarked that there are different possible definitions of “running-in”. Some authors suggest a running-in phase in which essentially the roughness is altered, and there is a departure from the later regime of “linear behavior”, described by the Reye–Archard law [Reye 1860; Archard and Hirst 1956]. Another interpretation of “running-in”, more relevant to the present paper, describes the phase where the pressure distribution changes in time due to elasticity effects. For a contact which changes pressure and also size in time, both phenomena may in principle be at work, but we shall concentrate in this paper on the second meaning of running-in, assuming the Reye–Archard law to apply throughout the process. It is perhaps interesting to remark that Reye’s work, though earlier, remained somehow unnoticed in the English-speaking literature, which tends to cite Archard’s work [Archard and Hirst 1956].¹ Both describe the dependence of worn volume V on normal load as linear and on hardness as inverse:

$$V = \frac{kPS}{HB}, \quad (1-1)$$

Keywords: wear, contact mechanics, finite element method, Archard wear law, Hertzian plane contact, transient wear.

¹As Villaggio [2001] says, “Reye’s model became very popular in Europe (in Italy was promulgated by Panetti [1947]), and it is still taught in university courses of applied mechanics. But, strangely enough, this theory has been totally ignored in English and American literature.”

where S is sliding distance, P is normal load, and HB is Brinell hardness. In this form, k is a dimensionless constant which, in the original Archard model, expresses the (unknown a priori) probability of an asperity to wear when sliding it by a length equal to twice its contact diameter (see also http://en.wikipedia.org/wiki/Archard_equation). It varies from about 10^{-2} for mild steel on mild steel to 2–3 orders of magnitude less for tool steels on metals, and even lower on plastic. Some values for ceramic on ceramic are as low as 10^{-6} . Notice that this law holds until the nominal pressure is lower than the yield. Above that, k grows with P , and hence we depart from linearity. Naturally, the many orders of magnitude of variation in k hide many possible changes of mechanisms and dependence on other constants, for example, toughness of the materials; and indeed the wear rate in certain ranges can increase, be independent of, or decrease with hardness depending on the particular toughness [Hornbogen 1975].

Often, as said before, running-in is associated to elasticity-dominated effects (see, for example, [Goryacheva 1998]). One class of problem is when the contact area is fixed in time, which permits special linear techniques to be used, like the eigenfunction expansion of the transient pressure distribution. However, another important class of problem does not neglect the change of contact area during the wear process, and hence cannot rely on linearity and the superposition principle.

Most of the present literature is concerned with FEM implementation of Archard's law (see, for example, [Mattei et al. 2011; Pödra and Andersson 1999; Sfantos and Aliabadi 2007]), and therefore the computational cost of a reasonably complex problem is significant. An approximate solution using the Winkler approximation for the contact, namely that the displacement is a local function of the pressure, is possible in closed form. In particular, here we extend the 2D treatment of [Goryacheva 1998] to provide full solutions also for pressure distribution. In common with Goryacheva, we shall assume wear is only acting on the indenter, and not in the half-plane. Finally, as a further extension, a section is added on an "adaptive" Winkler solution, in which the modulus is corrected for the changing contact area. This gives some hint of the degree of approximation of the solution. That the results with Winkler models can be very good compared to the full continuum problem is known in the literature (see, for example, [Pödra and Andersson 1997]).

2. General formulation

The problem we plan to solve is that of an elastic indenter that slides out-of-plane, over a Winkler half-plane. The indenter can also be elastic but, without loss of generality, we shall assume it is rigid. The half-plane is wearing much more slowly than the punch, so that we can neglect its wear process altogether. This is clearly not correct in general, but is a limit approximation when the wear coefficient of the indenter is much larger than that of the half-plane. If the contact repeats itself in some patterns, like in the case of a pin-on-disk situation, or pad-disk assembly, this amounts to assuming that wear of the disk is negligible compared to that of the pin or pad. The geometry and the symbols are described in Figure 1, where $d(t)$ is the indentation depth, $b(t)$ is the contact semiwidth, $u(x, t)$ is the displacement of the Winkler foundation, $w(x, t)$ is the indenter wear, and $g_0(x)$ is the initial gap function.

We shall consider the most interesting case, that of contact area growing in time, which is typical if the contact load is constant or increasing in time, although the more general cases of decreasing or variable loads require similar considerations (see, for example, [Goryacheva 1998] for the more general case).

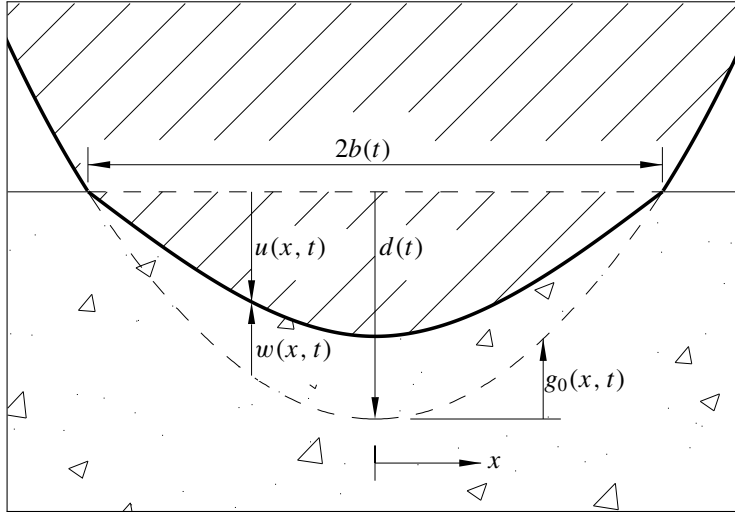


Figure 1. Indenter geometry and symbols. The figure takes into account the Winkler behavior for a contact area $2b(t)$ that is expanding in time. Triangles are used to indicate the elastic material in the half-plane.

2A. Formulation. With reference to [Figure 1](#), inside the contact area the displacement field is

$$u(x, t) = d(t) - g_0(x) - w(x, t). \tag{2-1}$$

As in the classical Winkler model, simple proportionality of pressure and displacement is assumed:

$$p(x, t) = k(t)u(x, t), \tag{2-2}$$

where $k(t)$ is the proportionality coefficient, or Winkler constant, having units of pressure per unit displacement—time-dependent in the most general formulation.

The Winkler model permits us to solve the pressure distribution in the contact area. In fact, inside the contact region, using (2-2) in (2-1) we have

$$p(x, t) = k(t)[d(t) - g_0(x) - w(x, t)]. \tag{2-3}$$

By integrating (2-3) over the contact length $[-b(t), b(t)]$, we find the state equation of the problem, which relates the contact evolution (constants b, d), the indenter wear, and the external load per unit length $P(t)$:

$$\frac{P(t)}{k(t)} = 2b(t)d(t) - \int_{-b(t)}^{b(t)} [g_0(x) + w(x, t)] dx. \tag{2-4}$$

2B. Indentation evolution. The profile wear is modeled by the Reye–Archard law. Hence, if $v(t)$ is the relative slip velocity, f is the friction coefficient, and β is the wear coefficient, we can write

$$\frac{\partial w(x, t)}{\partial t} = \beta f v(t) p(x, t) = \alpha(t) p(x, t), \tag{2-5}$$

where $\alpha(t) = \beta f v(t)$ is a parameter which takes into account the generally time-dependent velocity and $w(t)$ is the profile wear in the normal direction with respect to the contact area.

The indentation evolution $d(t)$ is obtained by differentiating (2-4) with respect to time. Using (2-5) and the condition that the edges of the contact region are progressively entering contact and hence have no wear, i.e., $w(b(t), t) = w(-b(t), t) = 0$, we find that

$$P'(t) = d'(t)2k(t)b(t) - \left[k(t)\alpha(t) - \frac{k'(t)}{k(t)} \right] P(t), \quad (2-6)$$

which can be easily integrated to give $d(t)$ and then $b(t) = g_0^{-1}[d(t)]$.

2C. Pressure field evolution. Let us now look at the pressure behavior at a fixed position \bar{x} ,

$$p(\bar{x}, t) = p(t).$$

The pressure field evolution is governed by (2-3). Differentiating it with respect to time and using (2-5), we find

$$p'(t) + \left[k(t)\alpha(t) - \frac{k'(t)}{k(t)} \right] p(t) = k(t)d'(t), \quad (2-7)$$

that is, a first-order ODE which can be solved by the variation of constants method, finding

$$p(t) = q(t)e^{-B(t)}, \quad (2-8)$$

where $B(t)$ is a general primitive of the coefficient,

$$B(t) = \int \left[k(t)\alpha(t) - \frac{k'(t)}{k(t)} \right] dt, \quad (2-9)$$

and where

$$q(t) = \int k(t)d'(t)e^{B(t)} dt + C, \quad (2-10)$$

with C an arbitrary constant of integration.

The initial condition to find the correct value of C depends on whether the particular value of \bar{x} is inside or outside the original contact area. In particular,

$$\begin{cases} \text{if } \bar{x} \in [-b(0), b(0)], \text{ then } p(\bar{x}, 0) = k[d(0) - g_0(\bar{x})]; \\ \text{else } p(\bar{x}, t) = 0 \text{ for } t < \bar{t}, \end{cases} \quad (2-11)$$

where \bar{t} is the time at which $|\bar{x}| = b(t)$.

3. Constant P, k, α

In order to develop analytical results, we will now focus on classical Hertzian indenters, although the approach to be described does not need any kind of limitation in terms of indenter geometry. The Hertzian indenter is characterized by its curvature radius R and

$$g_0(x) = \frac{x^2}{2R}. \quad (3-1)$$

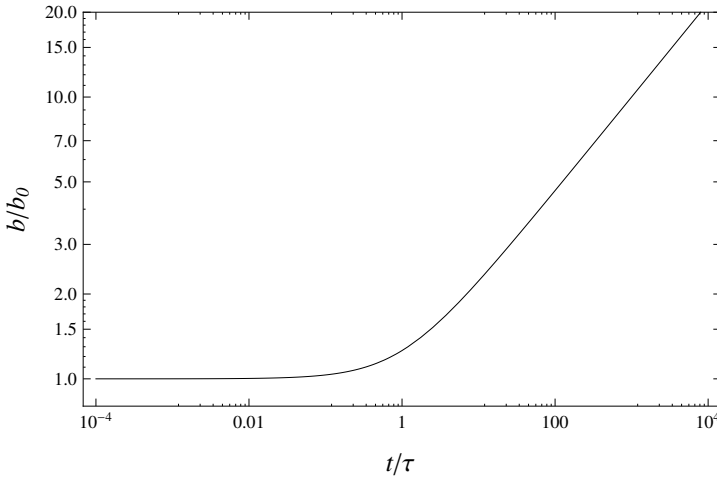


Figure 2. Dimensionless contact area vs. dimensionless time; b_0 is the initial contact area.

Assuming the load, the Winkler constant and the relative sliding speed between the indenter and the half-plane are all constant,

$$P(t) = P, \quad k(t) = k, \quad \alpha(t) = \alpha, \tag{3-2}$$

after some algebra (2-6) can be solved, finding

$$d(t) = \left(\frac{3P}{4k\sqrt{2R}} \right)^{2/3} (1 + \alpha kt)^{2/3}. \tag{3-3}$$

The initial condition depends on the Winkler constant k , but the steady state does not — and this explains the success of rigid models, which predict the steady state from purely kinematic considerations. For example, the design of brakes systems is classically based upon rigid models (see [Sfantos and Aliabadi 2007]). This important simplification is valid for every indenter shape described by $g_0(x)$, not only for the Hertzian case, but it requires the assumptions of constant normal load and constant relative sliding speed.

Further, by (3-1), the contact area evolution is

$$b(t) = \sqrt{2R} \left(\frac{3P}{4k\sqrt{2R}} \right)^{1/3} (1 + \alpha kt)^{1/3}, \tag{3-4}$$

and it is shown in Figure 2. The “cross-over” time is a characteristic time of the process defined as

$$\tau = \frac{1}{k\alpha}. \tag{3-5}$$

3A. Pressure field. The pressure field evolution is a little more complex to evaluate. Using the above assumptions, (2-10) can be solved by differentiating (3-3) in time, finding

$$q(t) = \frac{2\alpha k^2}{3} \left(\frac{3P}{4k\sqrt{2R}} \right)^{2/3} \int \frac{e^{\alpha kt}}{(1 + \alpha kt)^{1/3}} dt + C,$$

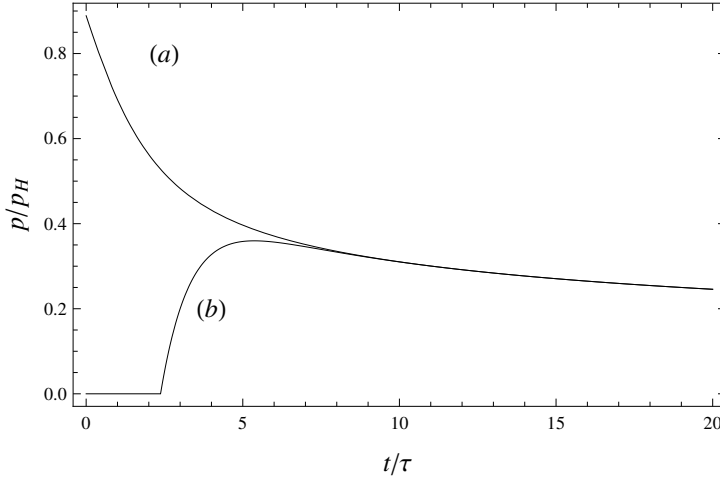


Figure 3. Pressure evolution vs. time. (a) $x = \frac{1}{3}b_0$ and (b) $x = \frac{3}{2}b_0$. Pressure values are nondimensionalized to the Hertzian initial peak pressure.

and the integral can be solved in terms of the exponential integral function:

$$\int \frac{e^{\alpha kt}}{(1 + \alpha kt)^{1/3}} dt = -\frac{(1 + \alpha kt)^{2/3} \text{Ei}_{1/3}(-1 - \alpha kt)}{\alpha ke}.$$

Therefore, according to (2-8), the pressure trend in time will be

$$p(t) = -\frac{2\alpha k^2}{3} \left(\frac{3P}{4k\sqrt{2R}} \right)^{2/3} \frac{(1 + \alpha kt)^{2/3} \text{Ei}_{1/3}(-1 - \alpha kt)}{\alpha ke} e^{-\alpha kt} + C e^{-\alpha kt},$$

where the initial condition C can be found by (2-11).

Figure 3 shows the pressure evolution in time for different fixed \bar{x} . As expected, inside the initial contact area (curve (a)) the pressure is monotonically decreasing and the reduction ratio is also monotonically decreasing. This is obviously due to the increase of the contact area in time because of wear. Outside the initial contact area, the pressure is initially zero (curve (b)), because the point is not yet in contact. When, due to wear of the indenter, contact occurs, the contact pressure suddenly increases. The pressure increase ratio is not only influenced by the rate of wear, but also by the local slope of the unworn profile which comes into contact. Both curves converge on the uniform pressure final stage.

4. The Winkler adaptive model

Winkler’s model can be applied to Hertzian contact as described in [Johnson 1985], which suggests that in our case a time-varying Winkler modulus can be defined by considering the time variation of the contact area and using the value suggested by Johnson which would give the best fit for the contact area semiwidth in the Hertzian case. Specifically,

$$k(t) = m \frac{E^*}{b_{ad}(t)} \text{ (plane contact),} \tag{4-1}$$

where $b_{ad}(t)$ is the semiwidth of the contact in our case, and $E^* = E/(1 - \nu^2)$ is the plain strain modulus. The numerical coefficient m can be chosen in order to match the initial Hertzian contact solution in terms of the contact semiwidth

$$b_{ad}(0) = a_H, \tag{4-2}$$

which gives $m = \frac{3\pi}{8}$, or the contact pressure peak

$$d_{ad}(0)k(0) = p_H, \tag{4-3}$$

which gives $m = \frac{8}{3\pi}$.

Hence, (2-6) becomes

$$d'_{ad}(t) = \frac{d_{ad}(t)P'(t) + mEd_{ad}^{1/2}(t)\alpha P(t)}{2\sqrt{2RmE} \left[d(t) - \frac{P(t)}{4mE} \right]}. \tag{4-4}$$

Following the procedure used in the main part of the paper, it is possible to evaluate the trend of penetration and contact area for constant normal load. After some algebra, we find that the implicit expression for penetration is

$$\frac{32R}{9\alpha^2 P^2} d_{ad}^3 - \frac{16R}{3P\alpha^2 mE} d_{ad}^2 + \frac{2R}{\alpha^2 m^2 E^2} d_{ad} = t^2.$$

In Figure 4, the contact semiwidth is plotted as a function of time for both adaptive (solid line) and constant (dashed line) Winkler modulus models. In particular, the results are obtained choosing the coefficient m according to (2-8). As expected, the behavior is different only at small times, while the long time limit does not depend on the Winkler stiffness, and thus the trend is the same.

The adaptive Winkler enhancement clearly affects the contact pressure evolution in time, which can be evaluated numerically by (2-7).

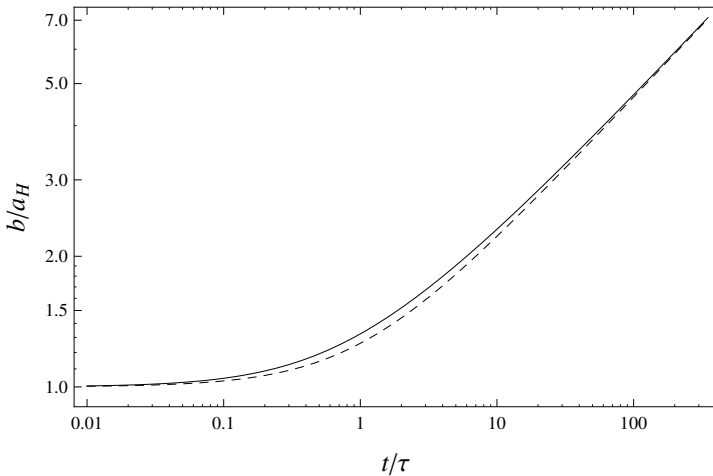


Figure 4. The comparison between contact semiwidths b obtained with constant (solid) and adaptive (dashed) Winkler models; a_H is the Hertzian contact semiwidth.

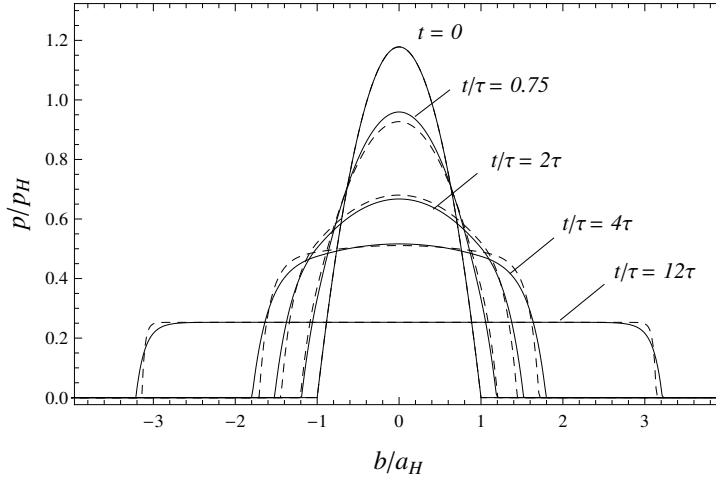


Figure 5. The pressure distribution inside the contact area for different times. Dashed lines give the solution obtained with constant Winkler modulus. Solid lines are obtained by introducing the adaptive Winkler model. The quantities p_H and a_H represent the Hertzian peak pressure and initial contact area.

Figure 5 shows this evolution in the cases of constant Winkler modulus (dashed line) and adaptive Winkler model (solid line). As in the Winkler approximation, the pressure distribution is proportional to the shape of indenter; the initial distribution is obviously parabolic, and as wear proceeds, the pressure distribution tends towards the uniform condition. It is also possible to see that the effect of the adaptive correction is to round the pressure distribution.

5. FEM comparison

A detailed comparison between simple and adaptive Winkler solutions and a FEM model was performed in order to study the accuracy of the Winkler solutions. In particular, we developed an ANSYS Parametric Design Language model of a half-cylinder with about 1000 elements. The contact between the cylinder and the rigid plane surface was modeled using CONTA178 elements, in which the gap of each element in contact is varied during the wear process by adding an artificial length corresponding to the progressive wear, proportional to the local pressure at the given iteration. This process corresponds to an Euler forward integration of the wear equations, and thus it was expected to be stable only for sufficiently small wear coefficient. To the best of the authors' knowledge, this FEM procedure has not been previously suggested. However, it is extremely simple to implement, does not require remeshing of the worn profiles, and in principle could be also used together with substructuring-superelement formulations in which only the degrees of freedom of the nodes in contact are active.

In Figure 6 the solutions of the Winkler models (dashed = simple, solid = adaptive) are compared to the FEM results (circles) for the contact area evolution as a function of time.

The adaptive Winkler model prediction clearly shows an improved fitting of FEM results compared with the simple Winkler model. In particular, after a brief time interval, the adaptive Winkler model

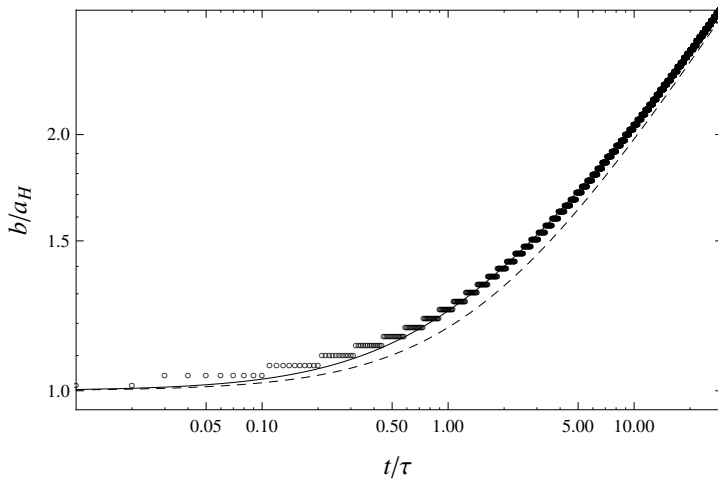


Figure 6. The dimensionless contact area semiwidth vs. the dimensionless time for different models. The circles are the FEM result, the solid line shows the adaptive Winkler result, and the dashed line shows the simple Winkler result.

correctly matches the solution obtained by FEM simulation in terms of contact area evolution, despite that the constants in the adaptive model are, strictly speaking, valid for a Hertzian pressure distribution.

Further, in [Figure 7](#), the pressure distribution within the contact area is shown for the Winkler models and the FEM elastic model, for a particular time $t/\tau = 0.8$. As expected, the adaptive Winkler model, while it improves the prediction of contact area size, is still somewhat far from the “exact” pressure distribution shape obtained by FEM simulations. However, this is intrinsic from the beginning, when the

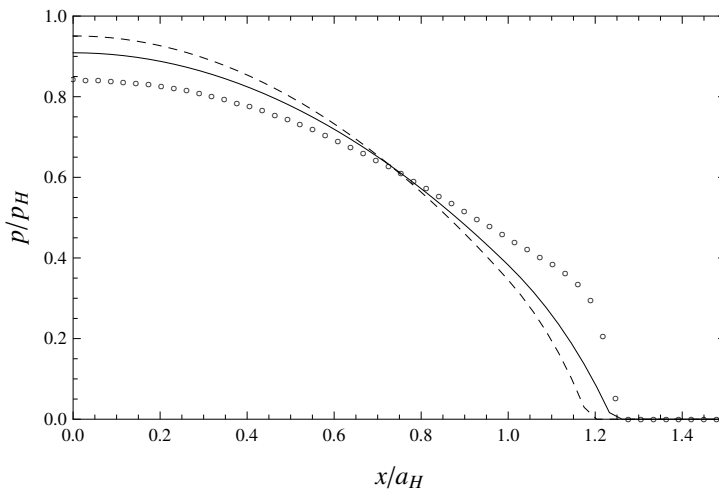


Figure 7. The dimensionless pressure distribution within the contact area at $t/\tau = 0.8$. The circles are the FEM result, the solid line shows the adaptive Winkler result, and the dashed line shows the simple Winkler result.

Hertzian elliptical distribution cannot match the parabolic Winkler distribution. In this respect, the error tends to be reduced from the initial value.

6. Conclusions

We have obtained some simple analytical results for 2D Hertzian rigid indenters sliding on a Winkler half-plane, on the assumption that only one of the bodies (the indenter) wears out. The full solutions for pressure distribution, contact area, and indentation depth have been obtained. The Winkler modulus can be also changed in time in an “adaptive” way, considering the varying dimension of the contact area, so as to improve the solution.

A comparison with a full continuum problem has been performed by means of FEM simulation using a very simple yet effective method to model wear, which adds wear in the “initial gap” of the contact elements. It is found that the introduction of the adaptive Winkler model improves the fixed load contact area prediction in time, and that generally the Winkler model shows a reasonable solution, considering the inevitable error intrinsic in the assumption of the pressure distribution shape.

References

- [Archard and Hirst 1956] J. F. Archard and W. Hirst, “The wear of metals under unlubricated conditions”, *Proceedings of the Royal Society of London A: Mathematical, Physical and Engineering Sciences* **236**:1206 (1956), 397–410.
- [Goryacheva 1998] I. G. Goryacheva, *Contact mechanics in tribology*, Solid Mechanics and its Applications **61**, Kluwer, Dordrecht, 1998.
- [Hornbogen 1975] E. Hornbogen, “The role of fracture toughness in the wear of metals”, *Wear* **33**:2 (1975), 251–259.
- [Johnson 1985] K. L. Johnson, *Contact mechanics*, Cambridge University Press, 1985.
- [Lim and Ashby 1987] S. C. Lim and M. F. Ashby, “Overview no. 55: Wear-mechanism maps”, *Acta Metallurgica* **35**:1 (1987), 1–24.
- [Mattei et al. 2011] L. Mattei, F. Di Puccio, B. Piccigallo, and E. Ciulli, “Lubrication and wear modelling of artificial hip joints: a review”, *Tribology International* **44**:5 (2011), 532–549.
- [Panetti 1947] M. Panetti, *Meccanica applicata*, Levrotto e Bella, Torino, 1947.
- [Pödra and Andersson 1997] P. Pödra and S. Andersson, “Wear simulation with the Winkler surface model”, *Wear* **207**:1–2 (1997), 79–85.
- [Pödra and Andersson 1999] P. Pödra and S. Andersson, “Simulating sliding wear with finite element method”, *Tribology International* **32**:2 (1999), 71–81.
- [Reye 1860] T. Reye, “Zur theorie der zapfenreibung”, *Der Civilingenieur* **4** (1860), 235–255.
- [Sfantos and Aliabadi 2007] G. K. Sfantos and M. H. Aliabadi, “Total hip arthroplasty wear simulation using the boundary element method”, *Journal of Biomechanics* **40**:2 (2007), 378–389.
- [Villaggio 2001] P. Villaggio, “Wear of an elastic block”, *Meccanica* **36**:3 (2001), 243–249.

Received 22 Jan 2014. Revised 14 Oct 2014. Accepted 25 Dec 2014.

MICHELE CIAVARELLA: mciava@poliba.it

Dipartimento di Meccanica, Matematica e Management, Politecnico di Bari, Viale Japigia 182, 70126 Bari, Italy

NICOLA MENGA: nicola.menga@poliba.it

Dipartimento di Meccanica, Matematica e Management, Politecnico di Bari, Viale Japigia 182, 70126 Bari, Italy

JOURNAL OF MECHANICS OF MATERIALS AND STRUCTURES

msp.org/jomms

Founded by Charles R. Steele and Marie-Louise Steele

EDITORIAL BOARD

ADAIR R. AGUIAR	University of São Paulo at São Carlos, Brazil
KATIA BERTOLDI	Harvard University, USA
DAVIDE BIGONI	University of Trento, Italy
YIBIN FU	Keele University, UK
IWONA JASIUK	University of Illinois at Urbana-Champaign, USA
C. W. LIM	City University of Hong Kong
THOMAS J. PENCE	Michigan State University, USA
DAVID STEIGMANN	University of California at Berkeley, USA

ADVISORY BOARD

J. P. CARTER	University of Sydney, Australia
D. H. HODGES	Georgia Institute of Technology, USA
J. HUTCHINSON	Harvard University, USA
D. PAMPLONA	Universidade Católica do Rio de Janeiro, Brazil
M. B. RUBIN	Technion, Haifa, Israel

PRODUCTION production@msp.org

SILVIO LEVY Scientific Editor

See msp.org/jomms for submission guidelines.

JoMMS (ISSN 1559-3959) at Mathematical Sciences Publishers, 798 Evans Hall #6840, c/o University of California, Berkeley, CA 94720-3840, is published in 10 issues a year. The subscription price for 2015 is US\$565/year for the electronic version, and \$725/year (+\$60, if shipping outside the US) for print and electronic. Subscriptions, requests for back issues, and changes of address should be sent to MSP.

JoMMS peer-review and production is managed by EditFLOW[®] from Mathematical Sciences Publishers.

PUBLISHED BY

 **mathematical sciences publishers**
nonprofit scientific publishing

<http://msp.org/>

© 2015 Mathematical Sciences Publishers

Special issue
In Memoriam: Huy Duong Bui

Huy Duong Bui	JEAN SALENÇON and ANDRÉ ZAOUÏ	207
The reciprocity likelihood maximization: a variational approach of the reciprocity gap method	STÉPHANE ANDRIEUX	219
Stability of discrete topological defects in graphene	MARIA PILAR ARIZA and JUAN PEDRO MENDEZ	239
A note on wear of elastic sliding parts with varying contact area	MICHELE CIAVARELLA and NICOLA MENGÀ	255
Fracture development on a weak interface near a wedge	ALEXANDER N. GALYBIN, ROBERT V. GOLDSTEIN and KONSTANTIN B. USTINOV	265
Edge flutter of long beams under follower loads	EMMANUEL DE LANGRE and OLIVIER DOARÉ	283
On the strong influence of imperfections upon the quick deviation of a mode I+III crack from coplanarity	JEAN-BAPTISTE LEBLOND and VÉRONIQUE LAZARUS	299
Interaction between a circular inclusion and a circular void under plane strain conditions	VLADO A. LUBARDA	317
Dynamic conservation integrals as dissipative mechanisms in the evolution of inhomogeneities	XANTHIPPI MARKENSCOFF and SHAIENDRA PAL VEER SINGH	331
Integral equations for 2D and 3D problems of the sliding interface crack between elastic and rigid bodies	ABDELBAÇET OUESLATI	355
Asymptotic stress field in the vicinity of a mixed-mode crack under plane stress conditions for a power-law hardening material	LARISA V. STEPANOVA and EKATERINA M. YAKOVLEVA	367
Antiplane shear field for a class of hyperelastic incompressible brittle material: Analytical and numerical approaches	CLAUDE STOLZ and ANDRES PARRILLA GOMEZ	395
Some applications of optimal control to inverse problems in elastoplasticity	CLAUDE STOLZ	411
Harmonic shapes in isotropic laminated plates	XU WANG and PETER SCHIAVONE	433